

Combined data from LDL composition and size measurement are compatible with a discoid particle shape

Tom Teerlink,^{1,*} Peter G. Scheffer,* Stephan J. L. Bakker,[†] and Robert J. Heine[†]

Departments of Clinical Chemistry* and Endocrinology,[†] Institute for Cardiovascular Research, VU University Medical Center, 1007 MB Amsterdam, The Netherlands

Abstract The size of LDL is usually reported as particle diameter, with the implicit assumption that it is a spherical particle. On the other hand, data obtained by cryoelectron microscopy and crystallographic analysis suggest that LDL shape may be discoid. We have investigated LDL particle geometry by combining data on LDL lipid composition with size measurement. The mean LDL diameter of 160 samples was measured by high-performance gel-filtration chromatography (HPGC), and particle volume was calculated from its lipid composition. Assuming a spherical shape, diameters calculated from volume correlated poorly with values obtained by HPGC ($R^2 = 0.36$). Assuming a discoid shape, particle height was calculated from volume and HPGC diameter. Diameter (20.9 ± 0.5 nm) and height (12.1 ± 0.8 nm) were not significantly related to each other ($r = 0.14$, $P = 0.09$) and accounted for 23% and 77%, respectively, of the variation in particle volume. In multivariate regression models, LDL core lipids were the main determinants of height ($R^2 = 0.83$), whereas free cholesterol in the shell, which contributes only 5–9% to LDL mass, was the main determinant of diameter ($R^2 = 0.54$). We conclude that combined data from composition and size measurements are compatible with a discoid particle shape and propose a structural model for LDL in which free cholesterol plays a major role in determining particle shape and diameter.—Teerlink, T., P. G. Scheffer, S. J. L. Bakker, and R. J. Heine. Combined data from LDL composition and size measurement are compatible with a discoid particle shape. *J. Lipid Res.* 2004. 45: 954–966.

Supplementary key words atherosclerosis • low density lipoprotein • low density lipoprotein composition • low density lipoprotein structure • low density lipoprotein size • unesterified cholesterol

Human LDL particles are the main carriers of cholesterol in the circulation. LDL particles are operationally defined as lipoproteins within the density range of 1.019–1.063 g/ml. As such, LDL forms a heterogeneous family

of particles varying in density, size, composition, and other physicochemical properties. This heterogeneity has clinical significance in that LDL subspecies differ in their metabolic behavior and pathologic roles [reviewed by Berneis and Krauss (1)]. During the last two decades, evidence has accumulated that LDL size is a parameter of particular clinical importance. Small, dense LDLs have consistently been shown to confer increased risk for cardiovascular disease (2–8). The presence of small, dense LDLs is strongly associated with increased plasma triglyceride (TG) levels and low HDL cholesterol, a triad collectively known as the atherogenic lipoprotein phenotype. The metabolic intertwining of these lipid risk factors makes it difficult to assess their independent contributions to cardiovascular risk. However, results from the Quebec Cardiovascular Study have demonstrated that small, dense LDLs are an important predictor for ischemic heart disease in men, independent from concomitant variation in plasma lipid concentrations (5, 6). It thus seems that information on LDL size improves the ability to predict cardiovascular disease risk over traditional lipid variables.

Several techniques can be used to measure LDL size and size distribution, such as electron microscopy of negatively stained lipoproteins (9), photon correlation spectroscopy using light-scattering equipment (10), proton nuclear magnetic resonance spectroscopy (11–13), high-performance gel-filtration chromatography (HPGC) (14, 15), and nondenaturing polyacrylamide gradient gel electrophoresis (GGE). The latter technique has been most widely used in clinical and epidemiological studies. It has a very high resolution, enabling the separation of up to

Abbreviations: apoB-100, apolipoprotein B-100; CE, cholesteryl ester; FC, free (unesterified) cholesterol; GGE, gradient gel electrophoresis; HPGC, high-performance gel-filtration chromatography; IDL, intermediate density lipoprotein; PL, phospholipid; TG, triglyceride.

¹To whom correspondence should be addressed.
e-mail: t.teerlink@vumc.nl

Manuscript received 22 December 2003 and in revised form 6 February 2004.

Published, JLR Papers in Press, February 16, 2004.
DOI 10.1194/jlr.M300521-JLR200

Copyright © 2004 by the American Society for Biochemistry and Molecular Biology, Inc.

This article is available online at <http://www.jlr.org>

seven or eight subclasses of LDLs (7, 16, 17). Most often, however, the so-called LDL peak particle diameter (i.e., the diameter of the most abundant LDL subclass within an individual) is reported. The use of the term diameter implies that LDL is a spherical particle. If LDL is envisioned as a stabilized oil-in-water emulsion, a spherical geometry is a logical consequence of the tendency of such emulsions to minimize the area of the oil droplets. Using an emulsion particle model, it has been shown that it is possible to predict the composition, density, and hydrodynamic properties of LDL as a function of particle size (18). Data obtained by electron microscopy with negative staining are also compatible with a spherical shape (9). Therefore, it is not surprising that a spherical particle shape is often taken for granted. On the other hand, there are strong indications, obtained by cryoelectron microscopy and crystallographic analysis, that LDL has a pseudocylindrical or discoid particle shape (19–24). There is yet another simple but compelling argument against spherical particle shape. If LDL consists of a spherical core surrounded by a 2 nm monolayer of polar lipids and protein, its diameter is expected to be mainly determined by the volume of its core. This would inevitably lead to a strong association between particle size and the cholesteryl ester (CE) content of LDL, because CE is the major core lipid. In contrast to this expectation, the strongest associations between particle size and lipid content are usually found for the polar surface-oriented lipids (14, 16, 25–27).

In the present study, we have attempted to differentiate between spherical and nonspherical particle geometry using the following strategy. The fact that each LDL particle contains a single copy of apolipoprotein B-100 (apoB-100) allows straightforward calculation of average LDL particle volume from its lipid composition (16, 18). If LDL is spherical, its mean diameter, as calculated from particle volume, should be in close agreement with the diameters obtained by direct measurement. We have measured average LDL size using an HPGC technique that is characterized by very high precision (14). Analysis of 160 LDL preparations revealed a poor correlation between LDL diameters measured by HPGC and calculated from volume, indicative of nonspherical geometry. Using a discoid particle model, the data could be reconciled. A direct consequence of a discoid LDL model is that two parameters (i.e., particle diameter and height) are required to characterize the particle. We have investigated the associations between these particle dimensions on the one hand and LDL lipid constituents and plasma lipids on the other hand. On the basis of our data, we present a structural model of LDL in which free cholesterol plays a major role as a determinant of particle shape and diameter.

METHODS

Samples

We used plasma samples from 160 subjects with well-controlled type 2 diabetes who were participating in ongoing trials at the Diabetes Center of the VU University Medical Center. The lo-

cal ethics committee approved these trials, and all subjects gave written informed consent. Subjects were selected to ensure a broad distribution of fasting plasma TGs. Fasting blood samples were collected into EDTA-containing tubes and centrifuged at 1,500 *g* for 10 min at room temperature. Plasma was stored at -70°C until analysis.

LDL isolation

LDL was isolated from 0.9 ml of plasma by ultracentrifugation between densities of 1.019 and 1.063 g/ml as described previously (14). Briefly, plasma was adjusted to a density of 1.019 g/ml and centrifuged at 417,000 *g* for 1 h, 40 min at 15°C in a Beckman Optima-TLX ultracentrifuge with a fixed-angle type 100.4 rotor. After removal of the top layer, containing VLDL and intermediate density lipoprotein (IDL), the density of the infranatant was adjusted to 1.063 g/ml, followed by centrifugation for 5 h at 417,000 *g*. Subsequently, LDL was collected from the top of the tube and stored at 4°C in the dark. From a limited number of samples, LDL was also isolated between densities of 1.031 and 1.044 g/ml. This narrow density range results in a more homogeneous LDL preparation, from which the buoyant LDL-1 and dense LDL-6 subfractions, as defined by Baumstark et al. (28), are excluded.

LDL particle size measurement

LDL size was measured by HPGC, essentially as described before (14), but with a modified calibration procedure. Isolated LDL samples (50 μl) were chromatographed on a Superose 6 column from Pharmacia (Uppsala, Sweden) at a flow rate of 0.5 ml/min with PBS (0.1 mol/l sodium phosphate, 0.2 mol/l NaCl, and 0.1 mmol/l EDTA, pH 7.4) as a mobile phase. Detection was performed at 280 nm. LDL eluted between 20 and 26 min as a nearly symmetrical peak, and the retention time of the peak apex was used to calculate average LDL particle diameter, using thyroglobulin and its dimer (17.0 and 23.6 nm, respectively) and fibrinogen (22.2 nm) as calibrators of known diameter. Using this HPGC system, the values obtained are strongly correlated with values measured by the widely used native GGE system ($r = 0.88$, $P < 0.001$). For quality control, an LDL sample stored in aliquots at -70°C was included in every series of samples. Intra-assay and interassay coefficients of variation for LDL diameter were 0.1% and 0.2%, respectively. Column temperature was kept at 25°C by means of a water bath. In some experiments, calibration of the column and determination of LDL size were performed at a temperature of 37°C .

LDL composition

Total cholesterol, free (unesterified) cholesterol (FC), phospholipids (PLs), and TGs in LDL were analyzed with commercially available tests (Roche, Mannheim, Germany) on a Cobas Bio centrifugal analyzer (Roche). Coefficients of variation for these assays are less than 2%. CEs were calculated as the difference between total cholesterol and FC. Because the method for the determination of PL is based on the detection of choline after enzymatic hydrolysis, it only detects choline-containing PL, i.e., (lyso)phosphatidylcholine and sphingomyelin. As LDL contains $\sim 7\%$ non-choline-containing PL (18), measured values were multiplied by 1.075. The protein content of LDL was measured by the Lowry method modified to allow measurement in lipoproteins, as described by Markwell et al. (29). Because apoB-100 leads to a more intense color development in the assay compared with BSA used for calibration, a correction factor has to be applied (16, 18, 28). To assess this factor, absolute protein determinations were performed by amino acid analysis of LDL samples ($n = 6$) after 24 h of hydrolysis at 110°C in 6 mol/l HCl. Amino acid analysis was performed by reversed-phase chromatography after precolumn derivatization with ortho-phthalal-

dehyde (30). The concentrations of leucine and phenylalanine, amino acids that are fully recovered under these hydrolysis conditions, were used to calculate the apoB-100 concentration by comparison with the known amino acid composition of apoB-100 (31). In this way, we found that the colorimetric protein determination leads to an overestimation of the apoB-100 concentration by a factor of 1.06, in close agreement with the values established by other investigators (16, 28). Analysis of representative LDL samples by SDS-PAGE revealed only a single protein band; therefore, no correction for the presence of proteins other than apoB-100 was made.

Analysis of the fatty acid composition of the various lipid classes of LDL was performed as described previously (32). Briefly, lipids were extracted by the procedure of Bligh and Dyer (33) and separated by thin-layer chromatography. Individual fatty acids in the CE, PL, and TG fractions were analyzed by capillary gas chromatography after transmethylation (34).

Calculation of particle size and density

Particle volume and mass of LDL were calculated from its lipid composition essentially as described by Schumaker, Phillips, and Chatterton (18). The molecular weights of CE, PL, and TG are dependent on the chain length and degree of unsaturation of their esterified fatty acids. For a subset of 100 LDL samples, the fatty acid profiles of these lipid classes were determined to obtain an accurate estimate of their average molecular weights. For CE, PL, and TG, mean (SD) molecular weights of 647.9 (0.9), 786.0 (4.0), and 859.2 (6.1) were obtained. As the standard deviations were very small, the average values were used for subsequent calculations on all 160 samples. For FC, a molecular weight of 386.7 was used. The measured lipid-protein ratios (mmol/g) of LDL were converted to mass ratios by multiplying with the molecular weight of the respective lipid. In this way, the mass percentage of protein in LDL was calculated, and using the molecular weight of apoB-100 (513,000), the molecular weight of LDL was derived. To correct for the fact that apoB-100 is glycosylated, a value of 33,340 was added, assuming a carbohydrate content of 6.5% (18). To obtain molar LDL volume, similar calculations were performed using specific volumes of 1.058, 1.021, 0.984, 1.102, 0.74, and 0.60 ml/g for CE, FC, PL, TG, protein, and carbohydrate, respectively (18). The volume of a single LDL particle was then calculated by division through Avogadro's number (6.023×10^{23}). It should be noted that in all calculations of particle geometry, the carbohydrate content of LDL was ignored because the sugar chains of apoB-100 extend into the aqueous phase and therefore were considered not to contribute to the volume of the LDL particle. The carbohydrate content of apoB-100 was only included in calculations of LDL molecular weight and particle density. Density calculated in this way is slightly lower than buoyant density, attributable to the fact that at high centrifugal force LDL particles are compressed more than the surrounding salt solution.

PL is located in the shell of LDL, whereas CE and TG are almost exclusively confined to the core. In contrast, FC is mainly located in the shell of LDL (FC-shell) but is also present in appreciable amounts in the core (FC-core), the relative distribution between these compartments being determined by the distribution coefficient K (i.e., FC-shell as weight percentage of shell lipids divided by FC-core as weight percentage of core lipids). For K , we used a value of 6 (35). The FC-shell/FC-core ratio can be calculated by multiplying K with the mass ratio of the shell and core compartments. To this end, we used an iterative procedure in which as a first approximation all FC was assumed to be present in the shell, resulting in a FC-shell/FC-core ratio of $K \times (\text{FC} + \text{PL}) / (\text{CE} + \text{TG})$, with all lipids expressed on a mass basis. From this ratio and the total amount of FC, both FC-shell and FC-core were computed. Using these values, a second ap-

proximation of the FC-shell/FC-core ratio was calculated as $K \times (\text{FC-shell} + \text{PL}) / (\text{FC-core} + \text{CE} + \text{TG})$. This procedure was repeated until the difference between the converging values obtained during successive iterations was negligible.

Considerations of particle geometry

If LDL is a spherical particle of volume V , its radius r or diameter d can be calculated from the following formula:

$$V = 4/3 \times \pi \times r^3 = 1/6 \times \pi \times d^3 \quad (\text{Eq. 1})$$

and particle area A can be calculated as follows:

$$A = 4 \times \pi \times r^2 = \pi \times d^2 \quad (\text{Eq. 2})$$

The increase of particle area as diameter increases by a small amount can be calculated by differentiating equation 2 with respect to d :

$$\partial A / \partial d = 2 \times \pi \times d \quad (\text{Eq. 3})$$

If LDL is envisioned as a discoid particle (i.e., a cylinder with volume V , area A , radius r , diameter d , and height h), then its volume can be calculated using the following mathematical formula:

$$V = \pi \times r^2 \times h = 1/4 \times \pi \times d^2 \times h \quad (\text{Eq. 4})$$

The surface area A consists of two components: the flat top and bottom surfaces and the curved lateral surface of the particle. If the sum of the areas of the top and bottom surfaces is denoted as A_{flat} and the area of the lateral surface is denoted as A_{curved} , then the following equations hold:

$$A_{\text{flat}} = 2 \times \pi \times r^2 = 1/2 \times \pi \times d^2 \quad (\text{Eq. 5})$$

$$A_{\text{curved}} = 2 \times \pi \times r \times h = \pi \times d \times h \quad (\text{Eq. 6})$$

The area increase of both the flat and curved surfaces of the particle as diameter or height increases by a small amount can be calculated by differentiating both equations 5 and 6 with respect to d and h :

$$\partial A_{\text{flat}} / \partial d = \pi \times d \quad (\text{Eq. 7})$$

$$\partial A_{\text{flat}} / \partial h = 0 \quad (\text{Eq. 8})$$

$$\partial A_{\text{curved}} / \partial d = \pi \times h \quad (\text{Eq. 9})$$

$$\partial A_{\text{curved}} / \partial h = \pi \times d \quad (\text{Eq. 10})$$

Calculation of average particle diameter from average particle volume using equation 1 leads to an overestimation of average particle diameter, attributable to the fact that volume is proportional to the third power of diameter. This effect is more pronounced when the size distribution is broad. To assess the magnitude of this effect in our experiments, we have performed computer simulations using an algorithm capable of generating random numbers with a normal distribution. A mean value of 19.9 nm and a SD of 0.6 nm (the actual values for particle diameters calculated from composition as reported in Table 3) were used. The algorithm created a total of 500 individual virtual particles. Mean particle diameter was 19.916 ± 0.586 nm (range, 18.15–21.62 nm), and mean particle volume was $4,147 \pm 366$ nm³ (range, 3,130–5,291 nm³). It should be noted that this range of volumes was close to the actual range we measured (3,311–4,836 nm³ as reported in Table 3). When the average particle volume was used to calculate the average particle diameter, a value of 19.933 nm was obtained, 0.017 nm higher than the real value obtained by averaging the individual diameters. This simulation shows that calculation of average particle diameter from average volume does indeed lead to an overestimation, although the effect is almost negligible.

TABLE 1. Composition of LDL expressed as lipid protein ratio and as number of lipid molecules per LDL particle

Variable	CE	FC	FC-Shell	FC-Core	PL	TG
Lipid protein ratio (mmol/g)						
Mean (SD)	2.99 (0.36)	1.15 (0.19)	0.93 (0.16)	0.22 (0.03)	1.61 (0.18)	0.39 (0.09)
P2.5	2.33	0.74	0.56	0.15	1.18	0.24
P97.5	3.76	1.49	1.23	0.29	1.94	0.61
Lipid molecules per LDL particle						
Mean (SD)	1,536 (186)	590 (97)	475 (81)	115 (17)	825 (90)	202 (47)
P2.5	1,196	377	289	75	607	124
P97.5	1,928	765	629	147	994	311
P97.5/P2.5	1.61	2.03	2.18	1.96	1.64	2.51

CE, cholesteryl ester; FC, free (unesterified) cholesterol; FC-core, FC in the core compartment of LDL; FC-shell, FC in the surface compartment of LDL; PL, phospholipid; TG, triglyceride. P2.5 and P97.5 indicate the 2.5th and 97.5th percentiles.

Statistical analysis

Data are reported as means and SD, with ranges as 2.5th and 97.5th percentiles. For the analysis of agreement between methods of measurement, we used the statistical methods and graphic representation suggested by Bland and Altman (36). Univariate associations between LDL dimensions and other variables were first examined by calculation of Pearson correlation coefficients. Significant predictors of diameter or height were then used in stepwise forward multiple linear regression analysis with criteria of $P < 0.05$ for entry and $P > 0.1$ for exit. The regression models were checked for their residuals to have a normal distribution and a constant variability across the range of fitted values.

RESULTS

LDL composition

As our aim was to study the relation between LDL composition and particle dimensions, it was important to study LDL preparations with a wide range of particle diameters. Because LDL size is inversely associated with plasma TG levels, the most convenient way to accomplish this is to select subjects with a wide range of fasting TGs. Type 2 diabetes mellitus is associated with increased plasma TG levels; therefore, we chose to isolate LDL from plasma of 160 subjects with type 2 diabetes with plasma TGs ranging from 0.5 to 5.6 mmol/l.

The composition of LDL was determined after isolation from plasma by sequential ultracentrifugation. Because each LDL particle contains a single copy of apoB-100, it is convenient to express the lipid composition of LDL on a

protein basis (i.e., as millimoles of lipid per gram of protein), as shown in **Table 1**. From these data and the molecular weights of the lipids and apoB-100, the number of lipid molecules per LDL particle was calculated. The results (Table 1) show that CE molecules are present in the highest numbers, followed by PL, FC, and TG. The variation of the amount of lipid molecules (i.e., the ratio between the 97.5th and the 2.5th percentiles) was lowest for CE and PL (1.61 and 1.64, respectively), somewhat higher for FC (1.96 and 2.18 for FC-core and FC-shell, respectively), and highest for TG (2.51).

To facilitate the comparison with data from the literature, we also expressed the lipid composition on a mass percentage basis (**Table 2**). In the data shown in the upper part of the table, the protein part of LDL was included in the calculation. Protein (i.e., apoB-100) accounted for 18–26% of particle mass. A strong disadvantage of this way of presenting the composition of LDL is that in small LDL particles, the single copy of apoB-100 accounts for a larger mass percentage compared with that in large LDL particles. Mass percentages of all lipids will thus decrease with decreasing particle size, obscuring possible relative changes among the lipids. We circumvented this problem by expressing the lipid content as a percentage of the total lipid mass of LDL, as shown in the bottom part of Table 2. Expressed in this way, the variation in lipid content was somewhat smaller compared with data expressed on the basis of total LDL mass (upper part of Table 2) or expressed as number of lipid molecules per particle (Table 1), with the notable exception of TG, which showed the largest variation if expressed as a percentage of lipid mass.

TABLE 2. Composition of LDL expressed as percentage of LDL mass and as percentage of LDL lipid mass

Variable	CE	FC	FC-Shell	FC-Core	PL	TG	Protein
Percentage of LDL mass							
Mean (SD)	38.3 (2.3)	8.8 (1.0)	7.1 (0.8)	1.7 (0.2)	25.0 (1.3)	6.8 (1.7)	21.2 (1.7)
P2.5	33.5	6.6	5.2	1.3	21.6	4.1	18.2
P97.5	42.6	10.5	8.6	2.0	26.9	11.0	26.0
P97.5/P2.5	1.27	1.59	1.65	1.54	1.25	2.68	1.43
Percentage of LDL lipid mass							
Mean (SD)	48.6 (2.6)	11.1 (1.1)	8.9 (1.0)	2.2 (0.2)	31.7 (1.4)	8.6 (2.2)	
P2.5	42.8	8.6	6.7	1.7	28.4	5.3	
P97.5	53.6	13.0	10.6	2.5	34.1	15.0	
P97.5/P2.5	1.25	1.51	1.58	1.47	1.20	2.83	

TABLE 3. Physical characteristics of LDL estimated from LDL lipid composition assuming a spherical particle shape

Variable	Volume	Core Volume	Shell Volume	Diameter	Molecular Mass	Density
		nm^3		nm	$\times 10^6$	g/ml
Mean (SD)	4,142 (351)	2,141 (210)	2,001 (161)	19.9 (0.6)	2.59 (0.21)	1.031 (0.005)
P2.5	3,311	1,703	1,596	18.5	2.10	1.022
P97.5	4,836	2,600	2,296	21.0	3.00	1.044
P97.5/P2.5	1.46	1.53	1.44	1.14	1.43	1.022

Physical characteristics of LDL

From the compositional data (Table 1), the molar mass of the LDL particle was calculated by multiplying the number of molecules of each component per particle with its molecular weight, followed by summation of the results. Division by Avogadro's number then yields LDL particle mass. In a similar way, LDL molar volume and volume per particle were calculated. With the premise that LDL is a spherical particle, its diameter was derived from its volume (equation 1) and its density from volume and mass. The results of these calculations are summarized in **Table 3**. The difference in volume between the largest and the smallest (i.e., the 97.5th and 2.5th percentiles) LDL particles was 46%, which translates to a 14% difference in diameter. The difference for particle mass between these extremes was somewhat smaller compared with volume (43% vs. 46%), because larger particles have a higher lipid content and hence a lower density.

Comparison of measured LDL diameters with values calculated from composition

The major aim of our study was to compare LDL dimensions calculated from its chemical composition as described above with values obtained by direct measurements. To this end, the LDL preparations obtained after ultracentrifugation were also subjected to HPGC, a fully automated chromatographic method for the measurement of average LDL diameter with high precision in large series of samples. The results of the comparison of the 160 LDL preparations by both methods are shown as a scatterplot in **Fig. 1A**. Although the results obtained by both methods showed a highly significant association, the correlation coefficient was rather low ($r = 0.60$, $P < 0.0001$), considering that both methods are supposed to measure the same variable. In **Fig. 1B**, the results of both methods are compared by plotting the difference between the values obtained by both methods against the average of both methods in a Bland-Altman plot. As can be seen, the LDL diameters measured by HPGC are on average 0.94 nm larger than the calculated diameters (95% limits of agreement 0.03–1.86 nm). The 1.83 nm range encompassed by the 95% confidence limits is close to the range of actual LDL diameters, indicating that the two methods cannot be used interchangeably.

LDL dimensions assuming a discoid particle shape

Theoretically, the lack of agreement between estimates of LDL size obtained by direct measurement and by calculation can be explained by high imprecision of either one

or both of the methods. However, as explained in detail in Discussion, imprecision of measurements is responsible for only a small part of the lack of agreement between both estimates of LDL diameter. An alternative explana-

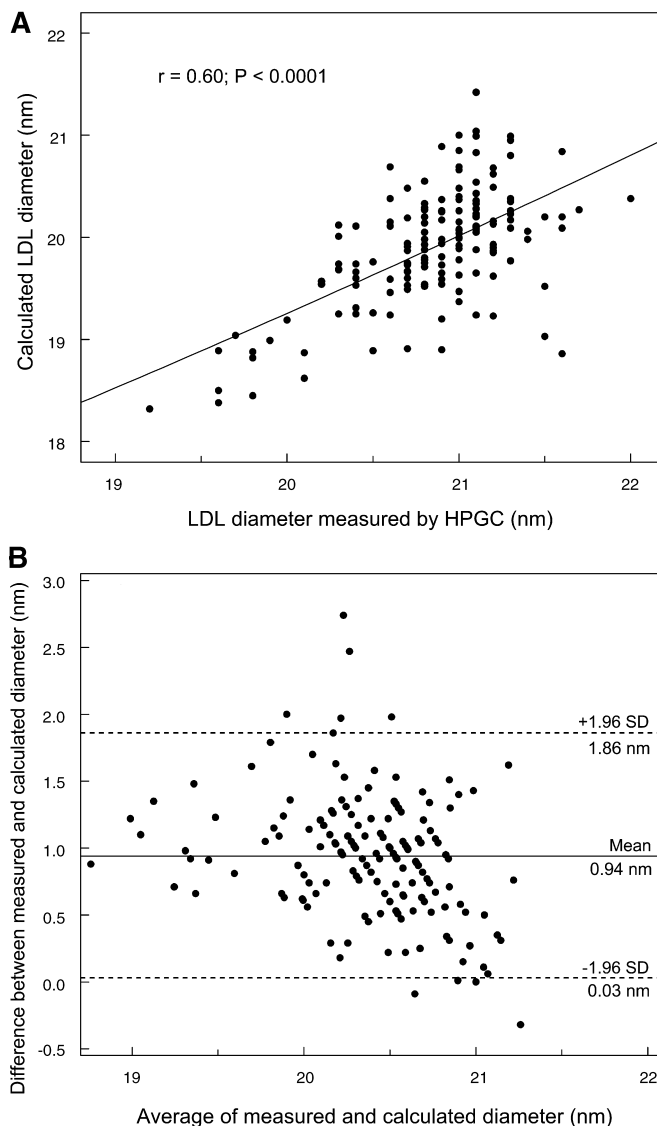


Fig. 1. A: Scatterplot of calculated LDL diameter versus measured diameter. LDL diameter was calculated from its volume as assessed from its lipid composition, assuming a spherical particle shape. LDL diameter measurement was performed by high-performance gel-filtration chromatography (HPGC). B: Bland-Altman plot of the difference between measured and calculated LDL diameters against the average of both estimates. The dotted lines indicate the 1.96 SD limits and encompass the 95% limits of the confidence interval.

tion is that the basic premise in calculating diameter from particle volume (i.e., that LDL is a spherical particle) is incorrect. We have explored whether our data on particle composition and size can be reconciled if a discoid particle shape is assumed. If LDL has the shape of a flat cylinder, its size and shape are defined by two parameters, the diameter and height of the cylinder, with diameter being larger than height. The latter restriction makes it reasonable to assume that in size determination by HPGC, diameter is the variable that is actually measured. The separation principle of HPGC is based on the capacity of LDL particles to diffuse into pores of the stationary phase. Whether a particle can enter a pore is determined by the largest dimension of the two-dimensional projection of the particle on the plane of the pore's orifice. In the case of a discoid particle, this largest dimension is equal to its diameter. As long as the condition that diameter is larger than height is satisfied, data obtained by the HPGC technique represent particle diameter. By combining LDL diameter with data on particle volume, calculated from its composition, it is now possible to calculate particle height (equation 4). The results of these calculations as given in **Table 4** show that mean particle height is much smaller than diameter (12.1 vs. 20.9 nm), which is reflected by the mean aspect ratio of 1.73. The prerequisite for this calculation to be valid (particle diameter should be greater than height, i.e., an aspect ratio of >1) was met for all LDL samples studied, as the aspect ratios ranged from 1.51 to 2.01. Variation of particle height was much larger than variation of particle diameter, as can be seen from the ratios between the highest and lowest values observed (**Table 4**) and from a scatterplot of the data (**Fig. 2**). Both size parameters were not significantly related to each other ($r = 0.14$, $P = 0.09$), and as indicated by the pairs of arrows in **Fig. 2**, subjects with LDL having the same diameter but widely differing heights and vice versa were present in the data set. Multiple regression analysis, with particle volume as the dependent variable, showed that height and diameter accounted for 77% and 23% of the variation in particle volume, respectively.

Influence of LDL density range on particle shape

LDL isolated between densities of 1.019 and 1.063 g/ml contains the complete spectrum from large, buoyant to small, dense particles. Mean particle diameters as measured by HPGC and values obtained by calculation from

TABLE 4. Dimensions of LDL assuming a discoid particle shape

Variable	Volume	Diameter	Height	Aspect Ratio
	nm^3	nm		
Mean (SD)	4,142 (351)	20.9 (0.5)	12.1 (0.8)	1.73 (0.12)
P2.5	3,311	19.6	10.5	1.51
P97.5	4,836	21.6	13.9	2.01
P97.5/P2.5	1.46	1.10	1.32	1.33

Volume was calculated from LDL composition, diameter was measured by high-performance gel-filtration chromatography, and height was calculated from volume and diameter. Aspect ratio represents the ratio of diameter and height.

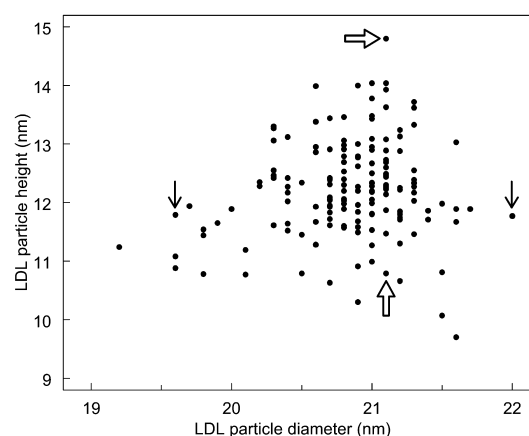


Fig. 2. Scatterplot of LDL particle height versus diameter. LDL diameter was determined by HPGC. Particle height was calculated from particle volume (calculated from its lipid composition) and diameter. Closed arrows indicate a pair of LDL samples with the same height (11.8 nm) but a 2.4 nm difference in diameter. Open arrows indicate a pair of LDL samples with the same diameter (21.1 nm) but a 4.0 nm difference in height.

particle volume may be influenced to a different extent by the actual size distribution. To investigate the importance of this possibly confounding factor, we also isolated LDLs between narrower density boundaries (1.031–1.044) from a limited number of samples ($n = 30$). Diameters obtained by HPGC measurement and diameters derived from composition, assuming a spherical particle shape, were rather poorly correlated ($r = 0.55$), similar to the results obtained for the 1.019–1.063 g/ml density range. Assuming a discoid particle shape, a mean diameter of 22.0 ± 0.3 nm (range, 21.5–22.5 nm) and a mean height of 11.8 ± 0.8 nm (range, 9.9–14.2 nm) were obtained, without significant correlation between the two dimensions ($r = 0.28$, $P = 0.14$).

Effect of temperature

We repeated the size measurement of the 1.031–1.044 g/ml density subfractions ($n = 30$) at 37°C to exclude the possibility that the discoid particle shape derived from our measurements is an artifact caused by the fact that size measurements were performed at 25°C (i.e., below the phase transition temperature of the core lipids). Particle diameters measured by HPGC at 37°C were closely correlated to values obtained at 25°C ($r = 0.95$, $P < 0.0001$) but were on average 0.21 ± 0.11 nm larger. Assuming a discoid particle shape, a mean diameter of 22.2 ± 0.3 nm (range, 21.7–22.8 nm) and a mean height of 11.6 ± 0.7 nm (range, 9.8–14.0 nm) were obtained, close to the values at 25°C.

Associations between LDL dimensions and lipid composition

Univariate associations between the lipid components of LDL and particle volume, diameter, height, and aspect ratio are shown in **Table 5**. The lipid composition was expressed as the number of molecules per particle. In this way, the mathematical entanglement of the individual lip-

TABLE 5. Univariate associations (Pearson correlation coefficients) between LDL lipid components and particle dimensions

Lipid Molecules per LDL Particle	Particle Volume	Core Volume	Shell Volume	Particle Diameter	Particle Height	Aspect Ratio
CE	+0.90	+0.94	+0.73	+0.46	+0.83	-0.66
FC	+0.83	+0.73	+0.88	+0.72	+0.60	-0.35
FC-core	+0.84	+0.83	+0.75	+0.62	+0.66	-0.45
FC-shell	+0.82	+0.69	+0.89	+0.73	+0.57	-0.33
PL	+0.92	+0.79	+0.98	+0.62	+0.75	-0.54
TG	+0.04	+0.03	+0.05	-0.08	+0.09	-0.13

Correlation coefficients shown in boldface are significant at $P < 0.0001$.

ids, resulting from expressing the lipid content as a mass percentage, was avoided. With the exception of TG, all lipid components showed strong and highly significant positive associations with particle dimensions and inverse associations with the aspect ratio. For TG, all associations were nonsignificant ($P > 0.1$).

To investigate which lipid components contribute the most to the dimensions of LDL, we examined these relations by multiple linear regression analysis. As particle volume and aspect ratio are by definition fully determined by the diameter and height of the particle, only regression models with the latter two as dependent variables were built. The resulting stepwise regression models for LDL diameter and height (Tables 6, 7) show that the lipids that independently contributed to diameter were different from the lipids that independently determined height. Particle diameter was to a large extent determined by the content of FC in the shell. Although the FC content of the core of LDL also entered the model, its contribution compared with FC-shell was negligible, as shown by the marginal increase of R^2 from 0.54 to 0.55 (Table 6). To investigate whether this model was critically dependent on the distribution of FC between the shell and the core, we examined the consequences of ignoring the distinction between FC-shell and FC-core (i.e., a stepwise regression analysis with CE, FC, PL, and TG as independent variables was performed). Only FC significantly contributed to the resulting model, which had a predictive power ($R^2 = 0.52$) that was almost equal to the model with FC-shell as the independent variable. In contrast to the models for diameter, FC did not contribute significantly to models of LDL height (Table 7). CE alone accounted for 69% of the variation in particle height, and after the addition of TG to the model, the explained variation increased to 83%.

TABLE 6. Stepwise multiple linear regression models with lipid components of LDL as determinants of LDL diameter

Model	Variable	β (95% CI)	Standardized β	P	Adjusted R^2	Residual SD
						<i>nm</i>
Model 1	FC-shell	0.0041 (0.0035–0.0047)	0.73	<0.0001	0.54	0.308
Model 2	FC-shell	0.0054 (0.0040–0.0068)	0.96	<0.0001		
	FC-core	-0.0066 (-0.0130–0.0002)	-0.25	0.045	0.55	0.305

CI, confidence interval. Variables allowed to enter the model were CE, FC-core, FC-shell, PL, and TG (as number of lipid molecules per LDL particle).

When samples were divided into two equal groups based on particle density (i.e., particles with a calculated density below and above the median), multivariate regression analysis gave essentially the same results (data not shown). Overall, we can conclude that the neutral lipids CE and TG, which reside in the core of the particle, are the main determinants of particle height, whereas the more polar lipid FC, which is mainly located in the shell of the particle, determines its diameter.

Next, we investigated multiple linear regression models with LDL diameter and height as determinants of the lipid content of LDL. The models for CE, FC-shell, FC-core, and PL content of LDL are summarized in Table 8. For TG, no significant model was obtained. The explained variance of the four models ranged from 78% to 88%. As can be seen from the standardized β values, particle height was the major determinant of CE content and to a lesser extent of PL and FC-core content, whereas diameter was the main determinant of FC-shell content.

The fact that both FC-shell and PL are confined to the shell of the particle that surrounds the core as a monolayer enabled us to calculate the increase in the number of these molecules per square nanometer increase of particle surface area from the regression coefficients of the respective regression models. Of note is the fact that as particle diameter increases, the flat top and bottom surfaces as well as the curved lateral surface of LDL increase in area (equations 7, 9). On the other hand, an increase in particle height leads only to an increase in the area of the lateral surface (equation 10), with no change in the area of the top and bottom surfaces (equation 8). This distinguishing geometrical feature of a cylinder allowed us to resolve the incremental surface density of PL and FC-shell into separate components for the flat and curved parts of the LDL particle. Surface densities calculated in this way were compared with incremental surface densities assuming a spherical geometry of LDL (Table 9). The surface density of PL is the same for the flat and curved surfaces and equals the density calculated for a spherical particle. In contrast, the incremental FC-shell density is much higher for the flat surfaces than for the curved surface. This is reflected by a much higher incremental FC/PL ratio of the flat surface (1.30 versus 0.71).

Association between particle dimensions and plasma lipids

Small, dense LDLs are a feature of the atherogenic lipid profile, together with increased plasma TGs and low HDL

TABLE 7. Stepwise multiple linear regression models with lipid components of LDL as determinants of LDL height

Model	Variable	β (95% CI)	Standardized β	<i>P</i>	Adjusted R^2	Residual SD
Model 1	CE	0.0037 (0.0033–0.0041)	0.83	<0.0001	0.69	<i>nm</i>
Model 2	CE	0.0043 (0.0040–0.0046)	0.96	<0.0001		0.46
	TG	0.0070 (0.0058–0.0082)	0.40	<0.0001	0.83	0.34

Variables allowed to enter the model were CE, FC-core, FC-shell, PL, and TG (as number of lipid molecules per LDL particle).

cholesterol. We have investigated whether the well-known positive correlation between LDL size and HDL cholesterol and the negative correlation between LDL size and plasma TGs are also apparent if LDL size is expressed in terms of particle volume, diameter, and height. The results shown in Fig. 3 demonstrate that the strongest associations with plasma TG were observed for LDL diameter, with weaker associations for LDL volume and height. Associations between LDL dimensions and HDL cholesterol showed the same trend but were in general less strong or even nonsignificant in the case of particle height.

DISCUSSION

The primary objective of this study was to determine whether or not LDL particle geometry is spherical. Our approach consisted of calculating particle volume from LDL lipid composition and measuring particle diameter by HPGC. If LDL is indeed a spherical particle, its diameter can be calculated from particle volume and the values obtained should be in good agreement with the values obtained by direct measurement. However, our results showed a large discrepancy between these two measures, suggesting that the assumption that LDL is spherical is false. Reconciliation of this discrepancy between direct size measurement and calculated values was obtained by assuming cylindrical particle geometry, necessitating the use of two parameters to describe particle size (i.e., diameter and height). This cylindrical model has some striking features. First, particle diameter was larger than particle height for all 160 samples studied, as can be seen from the aspect ratio (i.e., the ratio between diameter and height), which varied between 1.51 and 2.01. LDL thus resembles a flattened cylinder or disk. Second, height varied over a much wider range than diameter. The difference between the largest and smallest particles studied was 2.8 nm or 15% in terms of diameter, whereas the difference was 5.1

nm or 53% in terms of height. As a consequence, the variation in particle volume was mainly determined by variation in height and to a much lesser extent by variation in diameter. Linear regression analysis revealed that variations in height and diameter accounted for 77% and 23% of the variation in volume, respectively. Third, particle diameter and height seemed to be unrelated variables. Particles with extreme combinations of diameter and height were present in our data set (Fig. 2). This segregation between LDL dimensions was also apparent when we determined the main lipid determinants of diameter and height by multiple linear regression analysis. A salient feature of the models describing the associations between particle dimensions and lipid content is that particle height was primarily determined by the CE and TG content of LDL, whereas the FC-shell content of LDL was the main determinant of LDL diameter (Tables 6, 7). In other words, core lipids determine the height of the particle, whereas FC present on the surface determines its diameter. The latter association is remarkable given the fact that FC-shell accounts for only 5–9% of particle mass (Table 2). Other investigators have found this strong association between FC and LDL diameter as well (16, 26, 27).

It can be argued that the height dimension of LDL, introduced by us to account for the poor agreement between the two methods used to assess particle diameter, has no physical reality but is merely an artificial way to quantify the random scatter around the regression line between the size measurements shown in Fig. 1. Theoretically, the lack of agreement between estimates of LDL size obtained by direct measurement and by calculation can be explained by the high imprecision of either one or both of the methods. The precision of the HPGC method is very high (interassay coefficient of variation < 0.2%). The precision of the calculated diameters is somewhat lower, attributable to the fact that it is based on five measurements (CE, FC, PL, TG, and protein). However, the compositional data obtained in our study are in excellent

TABLE 8. Multiple linear regression models with LDL particle dimensions (diameter and height) as determinants of the number of lipid molecules per LDL particle

Variable	CE		FC-Shell		FC-Core		PL	
	β (95% CI)	Standardized β	β (95% CI)	Standardized β	β (95% CI)	Standardized β	β (95% CI)	Standardized β
Diameter (nm)	146 (117–174)	0.36	120 (107–133)	0.67	20 (17–22)	0.52	111 (100–122)	0.57
Height (nm)	175 (160–191)	0.78	50 (43–57)	0.51	14 (12–15)	0.65	71 (65–77)	0.66
Adjusted R^2 model	0.81		0.80		0.78		0.88	

TABLE 9. Incremental number of molecules of FC and PL per additional square nanometer of LDL surface area

LDL Particle Geometry	FC-Shell	PL	FC-Shell/PL Ratio
	<i>molecules/nm²</i>		
Spherical	0.93 ± 0.05	1.10 ± 0.04	0.85 ± 0.06
Discoidal			
Curved lateral surface	0.77 ± 0.06	1.08 ± 0.05	0.71 ± 0.06
Flat top and bottom surfaces	1.39 ± 0.10	1.07 ± 0.09	1.30 ± 0.15

The increase of total LDL surface area as particle diameter increases (see equations in Methods) was combined with the regression coefficients from Table 8 to calculate the incremental number of molecules per square nanometer of particle surface. Next, the incremental number of molecules on the curved lateral surface of the particle was calculated in a similar way from the regression coefficients and the increase of particle area with increasing height, based on the fact that the flat top and bottom surfaces of the particle do not change with particle height. The incremental number of molecules on the flat top and bottom surfaces was then calculated by subtraction. For comparison, data for a spherical LDL particle were calculated as well.

agreement with data reported by other investigators (16, 28, 37–40). In addition, during calculation of particle diameter, the relative measurement error is considerably attenuated, because diameter is proportional to the cubic root of particle volume (e.g., a 1.0% error in measurement of volume translates into a 0.33% error in calculated diameter). Finally, the fact that multivariate regression models showed the lipid components that independently determine LDL height to be different from the lipid components that determine LDL diameter strongly suggests that particle height is not a measurement artifact. Thus, the imprecision of measurements is probably responsible for only a small part of the lack of agreement between the two estimates of LDL diameter. We believe that this sufficiently shows that particle height is not a virtual dimension but is a real particle dimension.

There are some limitations to this study that deserve attention. First, it should be stressed that a discoid particle shape was not deduced from our experiments but was assumed a priori and shown to be compatible with our data. Our data could also be analyzed using an ellipsoidal model, in which particle shape is characterized by a long axis and a short axis. However, the ellipsoidal model would yield the same associations between lipid components and particle dimensions found for the discoidal model, with diameter and height replaced by long and short axes, respectively. Second, most of the HPGC measurements were performed at 25°C (i.e., below the phase transition of the lipid core). However, in a subset of samples, measurements performed at 37°C gave essentially identical results, suggesting that a discoid particle shape also represents the *in vivo* situation. Third, our results might be influenced by the fact that the LDL samples studied were all obtained from individuals with type 2 diabetes. It is known that the cluster of factors that constitute this metabolic syndrome is associated with small LDLs (41, 42). However, it has been shown that type 2 diabetes is not an independent determinant of LDL size; rather, its effects on LDL size are probably mediated via general metabolic processes involving TG-rich lipoproteins (37, 43). Therefore, we think that the results and implications of our study have general importance and are not limited to individuals with type 2 diabetes.

Our choice of a discoid model was based on data obtained by cryoelectron microscopy and crystallographic analysis, suggesting that LDL particles may have a pseudocylindrical or discoid shape (19–24). The particle dimensions derived from our model are in striking agreement with the values obtained by cryoelectron microscopy reported by van Antwerpen and colleagues (19, 21) (i.e., ~21 and 12 nm for diameter and height, respectively). These dimensions were derived from circular and rectangular projections of individual LDL particles in cryoelectron micrographs, in contrast to our study, in which average LDL dimensions for each subject were determined and no information on intraindividual heterogeneity of particle dimensions was obtained. Also, the wide range of aspect ratios, with an average value of ~1.7, reported by van Antwerpen et al. (22) closely agrees with the values observed in the present study.

An important question that remains to be answered is why LDL should adopt a discoid shape. As shown in Table 9, the incremental FC/PL ratio in the curved lateral surface of the particle is almost two times lower than that in the flat top and bottom surfaces. These differences between surface densities of the shell lipids may provide a clue to the driving force behind the transformation from spherical to discoid particle shape. In distearoylphosphatidylcholine liposomes, the surface area per PL molecule is ~65 Å² (44), close to the 62 Å² area reported for fully compressed monolayers of egg lecithin (35). As each PL molecule contains two acyl chains, the area per acyl chain amounts to 31–32.5 Å². In contrast, hydrocarbon chains in a crystalline lattice are much more densely packed to 18.5–20 Å² (i.e., ~60% of the area available for the PL acyl chains) (35). This shows that in planar monolayer or bilayer systems devoid of cholesterol, the PL acyl chains are loosely packed. In cholesterol-containing biological and artificial membranes, the sterol skeleton of FC interacts with the acyl chains of the PL molecules, resulting in condensation of the latter. In highly curved systems such as LDLs, the packing constraints experienced by the lipids attributable to geometrical restrictions perturb their physical properties and mutual interactions, in comparison with planar or less highly curved systems. A simple calculation may illustrate this. A spherical LDL particle of 20 nm

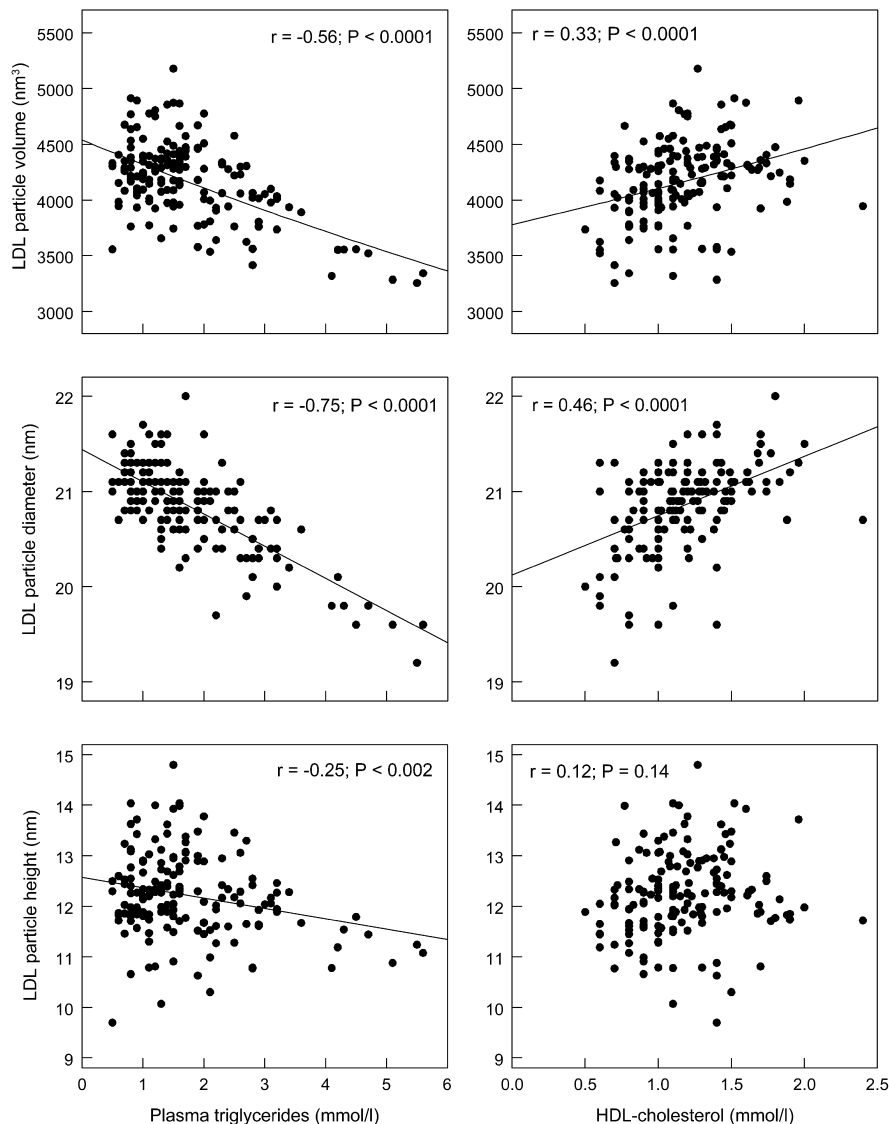


Fig. 3. Relations of LDL particle volume (top row), diameter (middle row), and height (bottom row) with plasma triglycerides (left column) and HDL cholesterol (right column).

diameter with a surface monolayer thickness of 2 nm has a core diameter of 16 nm. As the surface area is proportional to the square of the diameter, the ratio of the core to the surface area of the particle is $(16/20)^2 = 0.64$. The area available for the terminal methyl groups of the PL acyl chains residing at the interface between the surface monolayer and the core is thus only 64% of the area occupied by the PL head groups. This value is close to the area occupied by the acyl chains in a fully condensed state as estimated above, leaving little space for FC molecules between the PL acyl chains. If we consider a cylindrical LDL particle of 20 nm diameter, the situation is completely different. For the flat top and bottom surfaces, the ratio of the core to the surface area is 1, and for the lateral surface, being curved in only one dimension, the ratio of the core to the surface area is $16/20 = 0.8$. The space constraint arising in the surface monolayer of a spherical particle as its diameter gets smaller is thus relieved by the transition to a cylindrical configuration. This transition is

accompanied by a relative FC enrichment of the flat surfaces of the particle, leaving the curved lateral surface relatively devoid of FC, in accordance with the FC/PL ratios shown in Table 9. It is also possible that the distribution of FC between the shell and the core region of LDL is shifted toward the latter, or that some of the FC molecules leave the LDL particle altogether. Although we have shown that the shape transformation leads to a general relief of tension in the shell of the particle, we are left with a serious problem arising at the boundaries between the curved lateral surface and the flat top and bottom surfaces. There, the PL acyl chains meet at right angles, which is physically impossible. This boundary problem of our discoid LDL model can be resolved by assuming that both the upper and lower rims of the particle are covered by apoB-100. The model thus requires that the single apoB-100 molecule encircles the particle twice: once at the upper rim of the LDL particle and a second time at the lower rim of the particle. Assuming a diameter of 20 nm, a height of 12

nm, and a monolayer thickness of 2 nm, the core will have a diameter and height of 16 and 8 nm, respectively, requiring a minimal total path length of apoB-100 of $2 \times \pi \times 16 + 8 = 108$ nm. At first sight, this may seem an unrealistic value, much higher than the 65 nm length deduced from electron microscopy data of deoxycholate-solubilized apoB-100 reported by Gantz, Walsh, and Small (45) and also discordant with current models of LDL, in which apoB-100 fully encircles the spherical particle only once (46). In the belt-and-bow model put forth by Chatterton et al. (47), apoB-100 makes a full turn around the particle like a belt, with a loose C-terminal part crossing over and forming a bow. This model was very elegantly derived by measuring the angles between pairs of monoclonal antibodies directed against epitopes at defined positions in the primary structure of apoB-100 (47). However, the path followed by apoB-100 on the surface of LDL is not straight but meandering, and as observed by Hevonoja et al. (48) in their review of LDL structure, a total path length of 110–120 nm for apoB-100 can be derived from the data of Chatterton et al. (47). This value is close to the minimal path length derived from our discoid LDL model. In addition, apoB-100 is by necessity very flexible, as it must continually adapt its conformation and length to decreasing particle size during the lipolytic cascade from VLDL to LDL. This flexibility is in accord with data reported by McNamara et al. (16), who in a very elegant study of the particle composition and physical characteristics of eight LDL subspecies presented evidence that with decreasing particle size the core surface area requiring coverage by apoB-100 increases. Using a spherical particle model, they concluded that this expansion of apoB-100 across the core surface was accompanied by tertiary unfolding of the protein with a concomitant reduction of protein thickness. Thus, there are no indications that the total apoB-100 path length predicted from our discoid model is physically impossible.

The model described above explains why physical constraints in the surface monolayer force the particle to adopt a discoid shape. Although one is readily inclined to expect that flattening of LDL during the transition from spherical to discoid particle geometry must be accompanied by an increase in its diameter, this is not necessarily the case. It can be shown (by combining equations 1 and 4) that a spherical particle has the same volume and diameter as a cylindrical particle, with a height equal to two thirds of its diameter (i.e., with an aspect ratio of 1.5), slightly lower than the values observed in this study. Only if the cylindrical particle were further flattened beyond this point would an increase in diameter have to occur.

As expounded above, we believe that the FC content of the monolayer plays a crucial role in the transition from spherical to discoid particle geometry somewhere along the VLDL-IDL-LDL cascade. In addition, we want to take the crucial role of FC one step further by proposing that the FC content of LDL is responsible for the variation in particle diameter. Given that FC accounts for only 7–11% of LDL particle mass, it is not likely that the bulk of this lipid is responsible for the variation in particle diameter. A

hypothetical model explaining the strong association between FC and particle diameter is depicted in Fig. 4. If the FC content of the curved lateral particle surface is high, FC molecules are interspersed between the fatty acyl chains of the PL molecules, leading to a condensation of the surface monolayer. In this situation, the monolayer is a discrete compartment in which only the terminal methyl

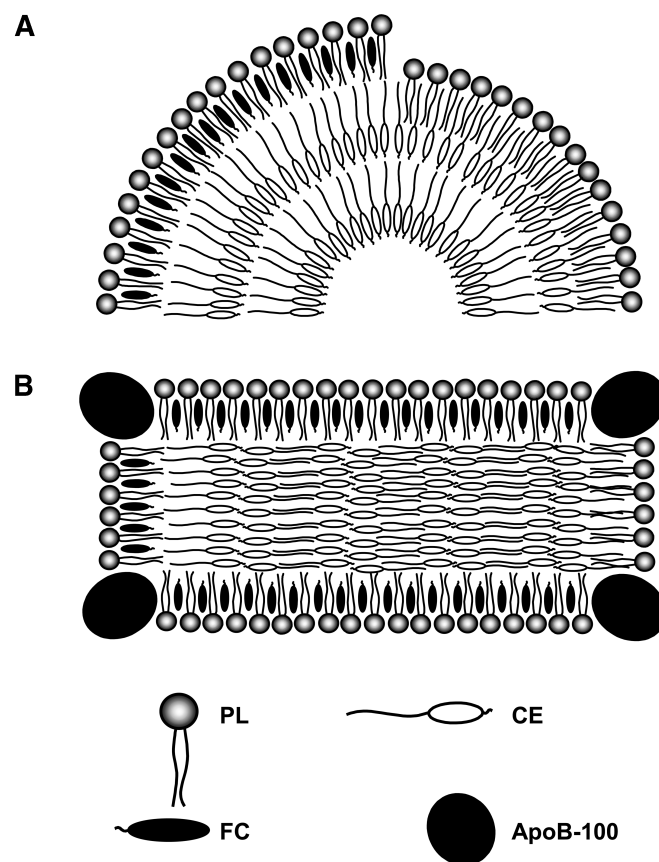



Fig. 4. Discoid model of LDL showing the crucial role of free cholesterol (FC) as a determinant of particle diameter. **A:** Part of a circular cross-section of the discoid LDL particle parallel to the flat surface. In the left part of the figure, the FC content in the curved lateral surface is high, leading to a condensed state of the outer monolayer. In this situation, the shell and core are distinct compartments. The right side of the figure shows the situation if the FC content of the particle shell is low, leading to a close interaction between the acyl chains of phospholipid (PL) molecules from the shell and the acyl chains of cholesteryl ester (CE) molecules from the core. In this situation, the distinction between separate shell and core compartments of the particle becomes diffuse and particle diameter decreases. The structure of the core is tentatively depicted to consist of two rings of CE molecules. **B:** Rectangular cross-section of the discoid LDL particle at right angles to the flat disk surface. In the left side of the figure, a condensed outer monolayer with a high FC content is shown. The right side of the figure shows a close interaction between the acyl chains of PL molecules from the shell and the acyl chains of CE molecules from the core, resulting from a low FC content of the shell. At the flat top and bottom surfaces, which are condensed as a result of their relatively high FC/PL ratio, the shell has little interaction with the core. The boundaries between the curved lateral surface and the flat top and bottom surfaces (i.e., the upper and lower rims of the particle) are covered by apolipoprotein B-100. The organization of the core is depicted to consist of a number of stacked layers of CE molecules.

groups of the PL acyl chains are in direct contact with the core. If the FC content of the monolayer decreases, its condensing effect on the acyl chains diminishes, leaving room for a closer interaction between the PL acyl chains and core lipids. In this state, the distinction between separate shell and core compartments becomes more diffuse as acyl chains from the surface PL molecules interdigitate with acyl chains from core CE molecules. The transition to this second state can be envisioned as the sinking of the PL acyl chains into the core. The estimated difference in particle diameter between these two extremes is ~ 3 – 4 nm, close to the range of diameters observed in this and other studies. This model offers an explanation for the strong association between LDL diameter and its FC content by assuming that the redistribution of FC between different LDL compartments (i.e., curved lateral surface, flat top and bottom surfaces, and core) can lead to changes in size by influencing the packing of lipids within the surface monolayer and their interaction with core lipids.

In the model shown in Fig. 4, we have tentatively depicted the structure of the core as consisting of two concentric rings of CE molecules. This layered structure is in accordance with the core model derived from small-angle X-ray scattering profiles and crystallographic analysis (24, 28, 48, 49). Although this organized core structure is generally believed to exist only below the phase transition temperature of the core lipids (46, 50), there are indications that the CE molecules also are restricted in their mobility at higher temperatures (49). In our discoid particle model, the overall shape of the particle may impose this restriction, forcing the CE molecules into stacks of planar layers, each consisting of two concentric rings. In this model, each layer contains a more or less fixed number of CE molecules, and the number of layers is proportional to particle height. This core structure explains the strong association between CE and particle height and the lack of association between CE and diameter in multivariate regression models.

Does our discoid particle model have any practical or clinical consequences? In this study, the associations of LDL size with HDL cholesterol and plasma TG were particularly strong for diameter. These associations were much weaker for height, whereas for particle volume, the strength of the associations was intermediate. In most studies that established an association between cardiovascular disease and LDL size, GGE was used to measure size. This technique, which is based on the capacity of particles to migrate through a mesh of pores of decreasing size, resembles the HPGC technique used in the present study in that it probably measures the largest dimension of the particle (i.e., diameter) with little influence of particle height. The close correlation between size measurements by both techniques corroborates this supposition (14). Other techniques, such as dynamic light scattering and NMR, in fact measure particle volume, from which diameter is calculated assuming a spherical particle shape. As the results of our study show that particle volume is more closely related to height than to diameter, results obtained by these techniques are not equivalent to results obtained by GGE or HPGC. The same reasoning holds for tech-

niques based on LDL density, such as density gradient ultracentrifugation, because density is inversely proportional to particle volume and is thus more closely related to height than to diameter. It is important to understand that volume-based techniques and diameter-based techniques in fact measure different physical properties of LDL and may yield complementary information. Combining the information obtained by both types of techniques in clinical studies may shed light on the metabolic and clinical relevance of the height dimension of LDL.

In summary, we have shown that the data from size measurement and lipid composition of LDL are compatible with a discoid particle model. A salient feature of this model is the crucial role assigned to FC in the shell of the particle, both in inducing the transition from spherical to discoid geometry and as a major determinant of particle diameter. An important consequence of the model is that techniques that are currently used to assess LDL size may not be equivalent, as some methods in fact measure particle volume instead of diameter. In conjunction with our observation that associations between plasma lipids and LDL dimensions are different for diameter and height, this suggests that the discoid particle model goes beyond an esoteric concept and may have metabolic and clinical significance. 

The authors thank Bert Volwater for technical assistance.

REFERENCES

1. Berneis, K. K., and R. M. Krauss. 2002. Metabolic origins and clinical significance of LDL heterogeneity. *J. Lipid Res.* **43**: 1363–1379.
2. Austin, M. A., J. L. Breslow, C. H. Hennekens, J. E. Buring, W. C. Willett, and R. M. Krauss. 1988. Low-density lipoprotein subclass patterns and risk of myocardial infarction. *J. Am. Med. Assoc.* **260**: 1917–1921.
3. Campos, H., J. J. Genest, Jr., E. Blijlevens, J. R. McNamara, J. L. Jenner, J. M. Ordovas, P. W. Wilson, and E. J. Schaefer. 1992. Low density lipoprotein particle size and coronary artery disease. *Arterioscler. Thromb.* **12**: 187–195.
4. Stampfer, M. J., R. M. Krauss, J. Ma, P. J. Blanche, L. G. Holl, F. M. Sacks, and C. H. Hennekens. 1996. A prospective study of triglyceride level, low-density lipoprotein particle diameter, and risk of myocardial infarction. *J. Am. Med. Assoc.* **276**: 882–888.
5. Lamarche, B., A. Tchernof, S. Moorjani, B. Cantin, G. R. Dagenais, P. J. Lupien, and J. P. Després. 1997. Small, dense low-density lipoprotein particles as a predictor of the risk of ischemic heart disease in men. Prospective results from the Quebec Cardiovascular Study. *Circulation.* **95**: 69–75.
6. Lamarche, B., A. C. St-Pierre, I. L. Ruel, B. Cantin, G. R. Dagenais, and J. P. Després. 2001. A prospective, population-based study of low density lipoprotein particle size as a risk factor for ischemic heart disease in men. *Can. J. Cardiol.* **17**: 859–865.
7. Williams, P. T., H. R. Superko, W. L. Haskell, E. L. Alderman, P. J. Blanche, L. G. Holl, and R. M. Krauss. 2003. Smallest LDL particles are most strongly related to coronary disease progression in men. *Arterioscler. Thromb. Vasc. Biol.* **23**: 314–321.
8. Vakkilainen, J., G. Steiner, J. C. Ansquer, F. Aubin, S. Rattier, C. Foucher, A. Hamsten, and M. R. Taskinen. 2003. Relationships between low-density lipoprotein particle size, plasma lipoproteins, and progression of coronary artery disease: the Diabetes Atherosclerosis Intervention Study (DAIS). *Circulation.* **107**: 1733–1737.
9. Forte, T. M., and R. W. Nordhausen. 1986. Electron microscopy of negatively stained lipoproteins. *Methods Enzymol.* **128**: 442–457.
10. O'Neal, D., P. Harrip, G. Dragicevic, D. Rae, and J. D. Best. 1998. A comparison of LDL size determination using gradient gel electrophoresis and light-scattering methods. *J. Lipid Res.* **39**: 2086–2090.

11. Otvos, J. D., E. J. Jeyarajah, D. W. Bennett, and R. M. Krauss. 1992. Development of a proton nuclear magnetic resonance spectroscopic method for determining plasma lipoprotein concentrations and subspecies distributions from a single, rapid measurement. *Clin. Chem.* **38**: 1632–1638.
12. Parks, J. S., and H. Hauser. 1996. Low density lipoprotein particle size and core cholesteryl ester physical state affect the proton NMR magnetic environment of fatty acid methylene and methyl nuclei. *J. Lipid Res.* **37**: 1289–1297.
13. Blake, G. J., J. D. Otvos, N. Rifai, and P. M. Ridker. 2002. Low-density lipoprotein particle concentration and size as determined by nuclear magnetic resonance spectroscopy as predictors of cardiovascular disease in women. *Circulation.* **106**: 1930–1937.
14. Scheffer, P. G., S. J. Bakker, R. J. Heine, and T. Teerlink. 1997. Measurement of low-density lipoprotein particle size by high-performance gel-filtration chromatography. *Clin. Chem.* **43**: 1904–1912.
15. Scheffer, P. G., S. J. Bakker, R. J. Heine, and T. Teerlink. 1998. Measurement of LDL particle size in whole plasma and serum by high performance gel-filtration chromatography using a fluorescent lipid probe. *Clin. Chem.* **44**: 2148–2151.
16. McNamara, J. R., D. M. Small, Z. Li, and E. J. Schaefer. 1996. Differences in LDL subspecies involve alterations in lipid composition and conformational changes in apolipoprotein B. *J. Lipid Res.* **37**: 1924–1935.
17. St-Pierre, A. C., I. L. Ruel, B. Cantin, G. R. Dagenais, P. M. Bernard, J. P. Després, and B. Lamarche. 2001. Comparison of various electrophoretic characteristics of LDL particles and their relationship to the risk of ischemic heart disease. *Circulation.* **104**: 2295–2299.
18. Schumaker, V. N., M. L. Phillips, and J. E. Chatterton. 1994. Apolipoprotein B and low-density lipoprotein structure: implications for biosynthesis of triglyceride-rich lipoproteins. *Adv. Protein Chem.* **45**: 205–248.
19. van Antwerpen, R., and J. C. Gilkey. 1994. Cryo-electron microscopy reveals human low density lipoprotein substructure. *J. Lipid Res.* **35**: 2223–2231.
20. Spin, J. M., and D. Atkinson. 1995. Cryoelectron microscopy of low density lipoprotein in vitreous ice. *Biophys. J.* **68**: 2115–2123.
21. van Antwerpen, R., G. C. Chen, C. R. Pullinger, J. P. Kane, M. LaBelle, R. M. Krauss, C. Luna-Chavez, T. M. Forte, and J. C. Gilkey. 1997. Cryo-electron microscopy of low density lipoprotein and reconstituted discoidal high density lipoprotein: imaging of the apolipoprotein moiety. *J. Lipid Res.* **38**: 659–669.
22. van Antwerpen, R., M. La Belle, E. Navratilova, and R. M. Krauss. 1999. Structural heterogeneity of apoB-containing serum lipoproteins visualized using cryo-electron microscopy. *J. Lipid Res.* **40**: 1827–1836.
23. Orlova, E. V., M. B. Sherman, W. Chiu, H. Mowri, L. C. Smith, and A. M. Gotto, Jr. 1999. Three-dimensional structure of low density lipoproteins by electron cryomicroscopy. *Proc. Natl. Acad. Sci. USA.* **96**: 8420–8425.
24. Lunin, V. Y., N. L. Lunina, S. Ritter, I. Frey, A. Berg, K. Diederichs, A. D. Podjarny, A. Urzhumtsev, and M. W. Baumstark. 2001. Low-resolution data analysis for low-density lipoprotein particle. *Acta Crystallogr. D Biol. Crystallogr.* **57**: 108–121.
25. Barter, P. J., O. V. Rajaram, H. Q. Liang, and K. A. Rye. 1993. Relationship between the size and phospholipid content of low-density lipoproteins. *Biochim. Biophys. Acta.* **1166**: 135–137.
26. Capell, W. H., A. Zambon, M. A. Austin, J. D. Brunzell, and J. E. Hokanson. 1996. Compositional differences of LDL particles in normal subjects with LDL subclass phenotype A and LDL subclass phenotype B. *Arterioscler. Thromb. Vasc. Biol.* **16**: 1040–1046.
27. Coresh, J., P. O. Kwiterovich, Jr., H. H. Smith, and P. S. Bachorik. 1993. Association of plasma triglyceride concentration and LDL particle diameter, density, and chemical composition with premature coronary artery disease in men and women. *J. Lipid Res.* **34**: 1687–1697.
28. Baumstark, M. W., W. Kreutz, A. Berg, I. Frey, and J. Keul. 1990. Structure of human low-density lipoprotein subfractions, determined by X-ray small-angle scattering. *Biochim. Biophys. Acta.* **1037**: 48–57.
29. Markwell, M. A., S. M. Haas, N. E. Tolbert, and L. L. Bieber. 1981. Protein determination in membrane and lipoprotein samples: manual and automated procedures. *Methods Enzymol.* **72**: 296–303.
30. Teerlink, T., P. A. van Leeuwen, and A. P. Houdijk. 1994. Plasma amino acids determined by liquid chromatography within 17 minutes. *Clin. Chem.* **40**: 245–249.
31. Cladaras, C., M. Hadzopoulou-Cladaras, R. T. Nolte, D. Atkinson, and V. I. Zannis. 1986. The complete sequence and structural analysis of human apolipoprotein B-100: relationship between apoB-100 and apoB-48 forms. *EMBO J.* **5**: 3495–3507.
32. Scheffer, P. G., S. J. Bakker, C. Popp-Snijders, R. J. Heine, R. B. Schutgens, and T. Teerlink. 2001. Composition of LDL as determinant of its susceptibility to in vitro oxidation in patients with well-controlled type 2 diabetes. *Diabetes Metab. Res. Rev.* **17**: 459–466.
33. Bligh, E. G., and W. J. Dyer. 1959. A rapid method of total lipid extraction and purification. *Can. J. Biochem. Physiol.* **37**: 911–917.
34. Popp-Snijders, C., and M. C. Blonk. 1995. Omega-3 fatty acids in adipose tissue of obese patients with non-insulin-dependent diabetes mellitus reflect long-term dietary intake of eicosapentaenoic and docosahexaenoic acid. *Am. J. Clin. Nutr.* **61**: 360–365.
35. Miller, K. W., and D. M. Small. 1987. Structure of triglyceride-rich lipoproteins: an analysis of core and surface phases. In *New Comprehensive Biochemistry*. Vol. 14. A. M. Gotto, Jr., editor. Elsevier Science Publications, Amsterdam. 1–75.
36. Bland, J. M., and D. G. Altman. 1995. Comparing methods of measurement: why plotting difference against standard method is misleading. *Lancet.* **346**: 1085–1087.
37. Lahdenperä, S., M. Syväne, J. Kahri, and M. R. Taskinen. 1996. Regulation of low-density lipoprotein particle size distribution in NIDDM and coronary disease: importance of serum triglycerides. *Diabetologia.* **39**: 453–461.
38. Galeano, N. F., R. Milne, Y. L. Marcel, M. T. Walsh, E. Levy, T. D. Ngu'yen, A. Gleeson, Y. Arad, L. Witte, M. Al-Haideri, S. C. Rumsey, and R. J. Deckelbaum. 1994. Apoprotein B structure and receptor recognition of triglyceride-rich low density lipoprotein (LDL) is modified in small LDL but not in triglyceride-rich LDL of normal size. *J. Biol. Chem.* **269**: 511–519.
39. Chen, G. C., W. Liu, P. Duchateau, J. Allaart, R. L. Hamilton, C. M. Mendel, K. Lau, D. A. Hardman, P. H. Frost, M. J. Malloy, and J. P. Kane. 1994. Conformational differences in human apolipoprotein B-100 among subspecies of low density lipoproteins (LDL). Association of altered proteolytic accessibility with decreased receptor binding of LDL subspecies from hypertriglyceridemic subjects. *J. Biol. Chem.* **269**: 29121–29128.
40. Chancharme, L., P. Thérond, F. Nigon, S. Lepage, M. Couturier, and M. J. Chapman. 1999. Cholesteryl ester hydroperoxide lability is a key feature of the oxidative susceptibility of small, dense LDL. *Arterioscler. Thromb. Vasc. Biol.* **19**: 810–820.
41. Hulthe, J., L. Bokemark, J. Wikstrand, and B. Fagerberg. 2000. The metabolic syndrome, LDL particle size, and atherosclerosis: the Atherosclerosis and Insulin Resistance (AIR) study. *Arterioscler. Thromb. Vasc. Biol.* **20**: 2140–2147.
42. Grundy, S. M. 1997. Small LDL, atherogenic dyslipidemia, and the metabolic syndrome. *Circulation.* **95**: 1–4.
43. Singh, A. T., D. L. Rainwater, S. M. Haffner, J. L. VandeBerg, W. R. Shelledy, P. H. Moore, Jr., and T. D. Dyer. 1995. Effect of diabetes on lipoprotein size. *Arterioscler. Thromb. Vasc. Biol.* **15**: 1805–1811.
44. Balgavý, P., M. Dubnicová, N. Kucerka, M. A. Kiselev, S. P. Yara-daikin, and D. Uhríková. 2001. Bilayer thickness and lipid interface area in unilamellar extruded 1,2-diacylphosphatidylcholine liposomes: a small-angle neutron scattering study. *Biochim. Biophys. Acta.* **1512**: 40–52.
45. Gantz, D. L., M. T. Walsh, and D. M. Small. 2000. Morphology of sodium deoxycholate-solubilized apolipoprotein B-100 using negative stain and vitreous ice electron microscopy. *J. Lipid Res.* **41**: 1464–1472.
46. Segrest, J. P., M. K. Jones, H. De Loof, and N. Dashti. 2001. Structure of apolipoprotein B-100 in low density lipoproteins. *J. Lipid Res.* **42**: 1346–1367.
47. Chatterton, J. E., M. L. Phillips, L. K. Curtiss, R. Milne, J. C. Fruchart, and V. N. Schumaker. 1995. Immunoelectron microscopy of low density lipoproteins yields a ribbon and bow model for the conformation of apolipoprotein B on the lipoprotein surface. *J. Lipid Res.* **36**: 2027–2037.
48. Hevonjoja, T., M. O. Pentikäinen, M. T. Hyvönen, P. T. Kovanen, and M. Ala-Korpela. 2000. Structure of low density lipoprotein (LDL) particles: basis for understanding molecular changes in modified LDL. *Biochim. Biophys. Acta.* **1488**: 189–210.
49. Atkinson, D., R. J. Deckelbaum, D. M. Small, and G. G. Shipley. 1977. Structure of human plasma low-density lipoproteins: molecular organization of the central core. *Proc. Natl. Acad. Sci. USA.* **74**: 1042–1046.
50. Coronado-Gray, A., and R. van Antwerpen. 2003. The physical state of the LDL core influences the conformation of apolipoprotein B-100 on the lipoprotein surface. *FEBS Lett.* **533**: 21–24.